

Stress Analysis of Perforated Plates Under Uniform Pressure

K.Kumar Chakradhar¹, B.Rama Krishna², A.Mahaboob Basha³

^{2,3} Assistant professor, Dept of Mechanical Engineering

^{1,2,3} Chiranjeevi Reddy Institute of Engineering and Technology, Anantapur, AP, India-515001

Abstract- The study predicted in this paper contains the numerical investigations on Perforated Plate (PP) as well as numerical and experimental investigations on Perforated Plate with Lining (PPL) which has a variety of applications in air and water engineering especially related to defense applications. Finite element method has been adopted as the tool for analysis of PP and PPL. The commercial software ANSYS has been used for static and free vibration response evaluation, whereas ANSYS LS-DYNA has been used for shock analysis. SHELL63, SHELL93, SOLID45, SOLSH190, BEAM188 and FLUID30 finite elements available in the ANSYS library as well as SHELL193 and SOLID194 available in the ANSYS LS-DYNA library have been made use of Unit cell of the PP and PPL which is a miniature of the original plate with 16 perforations have been used. Based upon the convergence characteristics, the utility of SHELL63 element for the analysis of PP and PPL, and the required mesh density are brought out. The effect of perforation, geometry and orientation of perforation, boundary conditions and lining plate are investigated for various configurations. Stress concentration and deflection factor are also studied. Based on these investigations, stadium geometry perforation with horizontal orientation is recommended for further analysis.

Keywords- Perforated plate, perforated plate with lining, Finite element analysis

I. INTRODUCTION

Plates are important structural elements in engineering applications such as pressure vessels, missiles, liquid containers, ship structures, and nuclear power equipments. The perforated plates are used in certain products because they are reducing weight and improve certain material properties. The perforated plates are used in the heat exchangers where these are called as tube sheets. The boiler is a well-known example for industrial application of the perforated plates. Their versatility includes screening, filtering, apportioning, ventilating, deflocculating, regulating, protecting, rasping, ordering and forming. The structural models are found in mechanical, civil, marine and aerospace structures. The structural cutouts are also used to provide ventilation and to alter the resonant frequency of the

structures. In addition to that the designers often need to integrate cutouts or openings in a structure to serve as doors and windows.

The holes in plate are arranged in various regular perforation patterns. Industrial applications include both square and triangular array perforation patterns. Behavior of the perforated component is drastically different from those of non-perforated component. Since the dynamic performance is always of interest, perforated rectangular plates having rectangular/triangular pattern with the circular/rectangular/square perforations are chosen and analytical, experimental models are formulated to find the fundamental frequency. The perforated plate analysis using finite element analysis technique by applying uni axial compressive loading using various patterns of the perforated sheets design is found out. The investigation is done with the help of Finite element analysis (FEA) and consequences. We found are nearer to investigational stress analysis. So, I adopted ANSYS software for analysis process. Then by using Finite element analysis (FEA) procedures diverse patterns are analyzed. Later this using Newton forward outburst technique estimate of results is completed for dissimilar patterns of holes on perforated. The hole pattern and in what way ought to be its direction under uniaxial firmness is tested. This paper also suggests which alignment should be used for minimum stress absorption at different hole patterns.

The paper transactions with stress analysis of plates perforated with holes organized in oblong plate with square pitch whole pattern. For this, in-plane masses are measured. Photo elasticity models stayed casted using photo elastic materials for rectangular plate with square pattern of holes. The analysis of perforated plates is done by using the Polaris cope in experimental method. The results found by experimental are likened with the Finite Element Method. From the experimental analysis for plate by means of circular, square and triangular cut out without bluntness, the stress absorption for circular cut out is less than the fair and triangular cut out and the stress concentration for square cut out is less than the triangular cut out. The stress concentration for triangular model is highest. By associating the results it is initiate that, the stress concentration by experimentation and

by FEM are in close agreement . The analysis of perforated plate has immediate application to tube sheet design.

However successful stress analysis required knowledge about elastic properties. Considerable effort has been directed towards their determination. However ASME has accepted the codes for the tube seats with triangular pitch pattern, but the codes standard for square pitch patterns have not been accepted so far. This is the motivation behind solving the present problem. Various design methods has been proposed by number of researchers for analyzing stress and deflection in multi perforated plates, properly known as tube sheets. The purpose for this dissertation work is to show the different techniques derived by various researchers in the analysis of perforated plates.

II. LITERATURE SURVEY

The presence of hole could reduce the ultimate strength and yield strength in a perforated plate. That's why the knowledge of stress concentration is very important to designers in solving many practical problems. A lot of work has been done in this field.

The problem or determination of stress concentration around a circular cut out in an infinite plate under tension was studied by Kirsch (1). He found that the stress concentration is maximum at a point on the hole boundary where the tangent to the hole boundary is parallel to the applied stress whereas at a point on the hole boundary, where tangent is perpendicular to the applied stress the stress concentration is minimum. The problem to determine the stress concentration in a semi-infinite plate with a circular hole under simple tension was investigated by Jeffery (2). Whereas Howland (3) determine the stress concentration around a circular hole in a plate of finite width under simple tension. When an increasing tensile load is applied to the ends of the plate the hole is positioned symmetrically in the plate width. Sokalov (4) determined the plastic zone around the circular hole in the case of biaxial tension. Fevebery (5) devised a technique to determine the plastic zone around a circular hole in the case of uniaxial tensile forces in a plate of finite dimensions. Thxsrir and Merketas (6) experimentally determined the elastic plastic stress and strain distribution occurring in a thin strip of a strain-hardening alloy with a central hole under uniaxial tension. Stresses were evaluated by introducing the assumption of plane stress in a material conforming to the misses yield criteria and the incremental flow stress strain relation. Maroal (7) used elastic finite element methods to determine the size of the plastic zones developing around the notches. Griffith (8) also estimated the elastic plastic deformation in edge notched tensile specimen under plane

stress condition by the finite element method. Ibrahim and Mcchallian (9) investigated on elastic plastic deformation around a circular hole in a plate under cyclic loading. Cookerhers and Baton (10) have derived a method to estimate the size of the plastic zone developing around the central hole in a finite width plate subjected to plane stress condition and to be made from elastic, linearly strain hardening material.

III. DESCRIPTION OF FINITE ELEMENTS

A brief description of the finite element in the library of ANSYS used in the present analysis has been given subsequently.

SHELL63 element

SHELL63 has both bending and membrane capabilities. Both in-plane and normal loads are allowable. The element has six degrees of freedom at each node: translations in the x, y, and z paths and rotations about the x, y, and z-axes. Stress stiffening and large bend capabilities are convoluted. The geometry, node positions and the synchronize system are shown in Figure.1. The element, by this thickness input at the 4 nodes. If the element has a constant thickness, only the thickness at one node resolves is input. Pressures would be input as the element faces on surface loads. Positive pressures act into the element. Nodal displacements and pressures, in-plane element forces, stresses and strain are the output of SHELL63.

SHELL93 element

SHELL93 is the element well suited to model curved shells. The geometry, node locations and the coordinate system are shown in Figure.2. The element has six degrees of freedom at each node. The deformation shapes are quadratic in both the in-plane directions. The element may have variable thickness capabilities.

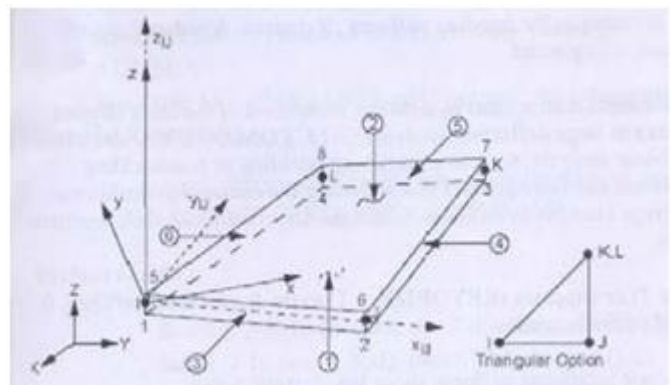


Figure. 1: Geometry & kinematics of SHELL63

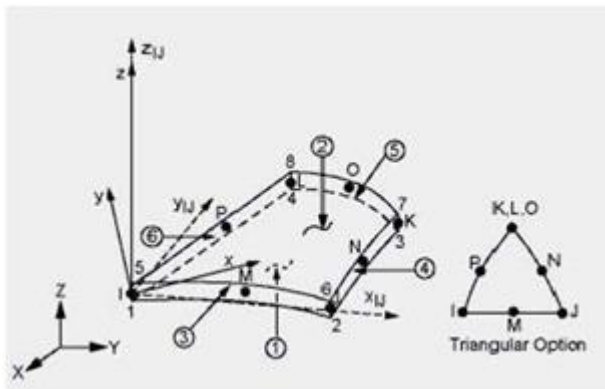


Figure.2:Geometry & kinematics of SHELL93

SOLID45 element

This element is used for the 3D modeling of solid structures. The element is defined by eight nodes having three degrees of freedom at each node viz., translations in the nodal x, y, and z directions. The element has plasticity, creep, swelling, stress stiffening, large deflection, and large strain capabilities. Reduced integration option with hourglass control is available.

SOLSH190 element

SOLSH190 is a solid element with added equations built-in to agree it to do a better job at computing bending in a thin section consuming unbiased one element concluded the thickness than a consistent solid element such as SOLID185.

SOLSH190 is used for simulating shell structures with a wide range of thickness (from thin to moderately thick). The element possesses the continuum solid element features eight- node connectivity with three degrees of freedom at each node: translations in the nodal x, y, and z directions. Thus, connecting SOLSH190 with other continuum elements requires no extra efforts .You can't use SOLSH190 for general determination meshing since the bending equations are created with situation to the thin Z-axis of the element. That means while meshing, you have to control the Z- axis of each element. That entails extra effort with universal purpose meshing.

Table 1: Element features

Element Description	Element name	No. of nodes	DOF at each node	Loading	Deformation shape
SHELL63	Elastic shell	4	6 (Ux, Uy, Uz, θx, θy, θz)	Pressure	Linear
SHELL93	8 node Structural shell	8	6 (Ux, Uy, Uz, θx, θy, θz)	Pressure	Quadratic
SOLID45	3-D Structural Solid	8	3 (Ux, Uy, Uz)	Pressure	Linear
SOLSH190	3-D 8 node Solid Shell	8	3 (Ux, Uy, Uz)	Pressure	Linear

IV. RESULTS & DISCUSSIONS

The deflection, von Mises stress and maximum principal stress are arrived for various configurations of unit cell shown in Table 2. The deflection obtained for NPP using finite element analysis for SOLID45 and SOLSH190 are found to be same for the respective mesh density.

Table 2: Details of finite element model and static structural responses of various configurations of unit cell of perforated plate with lining for pressure of 1Pa.

Configuration	Element	BC	Mesh density	Number of nodes	Number of elements	at Centerd				
						Deflection x 10 ⁻⁶ m	von Mises Stress Pa	Max. Principal Stress Pa		
SPP	SHELL63	BC3	78 x 156	23818	24784	0.1241	60.82	68.63		
	SHELL93			76426	24784	0.1362	72.44	78.60		
	SOLID45			69234	48808	0.1362	73.33	79.92		
	SOLSH190	69234		48808	0.1653	67.98	73.22			
	SHELL63	BC4		23818	24784	0.1624	63.22	71.56		
	SHELL93			76426	24784	0.1763	73.76	80.24		
SOLID45	19110		18288	0.2072	114.13	117.32				
SVP	SHELL63	BC3	84 x 110	36322	18288	0.2487	147.96	142.11		
	SHELL93			63442	46456	0.2493	149.82	144.32		
	SOLID45			63442	46456	0.2458	141.33	133.08		
	SOLSH190	19110		18288	0.2221	116.87	120.72			
	SHELL63	BC4		36322	18288	0.2390	149.68	146.24		
	SHELL93			11304	10848	0.1301	33.36	62.77		
SOLID45	33370		18848	0.1492	67.93	68.74				
EPP	SHELL63	BC3	47 x 112	26976	17792	0.1471	61.36	68.17		
	SHELL93			26976	17792	0.1473	61.34	68.07		
	SOLID45			11304	10848	0.1363	39.41	67.40		
	SOLSH190	33370		10848	0.1631	62.80	69.32			
	SHELL63	BC4		27398	26608	0.2038	100.21	104.32		
	SHELL93			81818	26608	0.2441	124.63	123.17		
SOLID45	81030		36932	0.2446	123.83	124.62				
EVP	SOLSH190	BC3	92 x 138	81030	36932	0.2610	116.81	112.44		
	SHELL63			27398	26608	0.2208	102.61	107.41		
	SOLID45			81818	26608	0.2441	124.63	123.17		
	NPP	SHELL63		BC3	70 x 130	18402	18200	0.0901	48.23	33.48
		SHELL93				33402	18200	0.0923	48.24	33.32
		SOLID45				33506	43300	0.0946	48.21	33.41
SOLSH190		33506	43300	0.0946		48.21	33.41			
SHELL63		BC4	18402	18200		0.1207	53.73	64.23		
SOLID45			33402	18200		0.1040	39.41	33.03		

Effect of perforation orientation

The variation in structural responses due to addition of 1mm lining plate is compiled and presented in Table 3. The response obtained from the analysis of PPL has been modified with COA and shown in this table so as to facilitate the comparison of this response with that of PP. It is observed that for BC3, the deflection is reduced by 35 to 50% and for BC4, deflection is reduced by 85%. For BC3, VMS is reduced by 15 to 27% and for BC4; the stress is reduced by 60%. For BC3, MPS is reduced by 10 to 34% and for BC4, it is reduced by 65%..

Table 3: Effect of lining plate on static structural responses for various configurations of unit cell in terms of percentage

Confg. Element	BC	Mesh density	as Convoid for 1Pa			as Convoid for (1 X 0.5448) Pa			% Variation in Def due to lining (PPL-PP)/PP*100	% Variation in VMS due to lining (PPL-PP)/PP*100	% Variation in SPS due to lining (PPL-PP)/PP*100		
			Deflection $\times 10^{-6}$ m	von Mises Stress, Pa	Min. Principal Stress, Pa	Deflection $\times 10^{-6}$ m	von Mises Stress, Pa	Min. Principal Stress, Pa					
SHP	BC3	76x156	SHELL63	0.1432	60.83	68.64	0.0791	33.14	37.39	-34.8	-13.1	-14.8	
			SHELL93	0.1677	72.42	79.61	0.0914	39.47	42.93	-34.4	-23.2	-20.5	
			SOLID45	0.1673	73.34	79.93	0.0911	39.96	43.53	-33.8	-21.2	-19.0	
			SOLSH190	0.1634	67.99	73.24	0.0901	37.04	39.90	-33.7	-22.0	-19.8	
	BC4	76x156	SHELL63	0.1635	63.23	71.57	0.0935	34.43	39.00	-36.6	-42.0	-42.8	
			SHELL93	0.1766	73.77	80.22	0.0962	40.19	43.72	-37.7	-46.4	-47.6	
			SHELL63	0.2073	114.16	117.33	0.1129	62.20	63.92	-39.8	-6.8	-11.4	
			SHELL93	0.2488	147.97	142.10	0.1335	80.61	77.42	-41.2	-13.9	-18.1	
	SVP	BC3	84x110	SHELL63	0.2494	149.83	144.33	0.1329	81.63	78.74	-40.2	-13.2	-16.2
				SOLID45	0.2489	141.34	133.09	0.1340	77.00	72.51	-40.2	-13.5	-16.1
				SHELL93	0.2250	116.88	120.76	0.1226	63.63	63.79	-38.4	-33.8	-39.7
				SOLSH190	0.2391	149.69	146.23	0.1412	81.33	79.68	-36.3	-61.4	-64.3
BC4		84x110	SHELL63	0.1302	33.37	62.78	0.0709	30.27	34.50	-41.3	-30.3	-39.6	
			SHELL93	0.1493	67.04	60.75	0.0813	36.52	33.10	-40.2	-36.3	-37.8	
			SOLID45	0.1472	61.27	68.18	0.0802	33.33	37.14	-40.0	-32.4	-30.5	
			SOLSH190	0.1474	61.33	68.08	0.0803	33.42	37.90	-36.3	-34.0	-31.1	
BC3		47x112	SHELL63	0.1564	39.40	67.41	0.0822	32.36	36.72	-37.6	-48.4	-48.8	
			SHELL93	0.1630	62.81	69.53	0.0888	34.22	37.88	-39.1	-71.9	-72.4	
			SHELL63	0.2039	100.20	104.33	0.1111	54.29	56.84	-39.1	-19.4	-23.7	
			SHELL93	0.2440	124.86	123.18	0.1329	68.02	67.11	-31.3	-34.9	-38.0	
BC4	47x112	SHELL63	0.2447	123.36	124.63	0.1333	68.41	67.88	-39.6	-32.2	-26.7		
		SOLID45	0.2611	116.80	112.45	0.1422	63.63	61.26	-47.2	-28.3	-33.7		
		SOLSH190	0.2209	102.60	107.42	0.1203	55.90	58.52	-36.6	-40.9	-44.2		
		SHELL93	0.2440	124.86	123.16	0.1329	68.02	67.10	-38.6	-46.3	-49.4		

Effect of perforation orientation

The effect of orientation of perforation has been studied independently for slotted and elliptical geometries and the details are compiled and presented in Table 4. In case of slotted perforation, it is observed that deflection for BC3 is reduced by 55 to 65% in SHP compared to that of SVP. In BC4, the deflection for SHP is reduced by 26 to 33%. For SHP for BC3, the VMS is reduced by 70% for SHELL63 whereas for other elements the stress is reduced by about 85%. For BC4, the VMS in SHP are reduced by about 58 to 76%. Similar changes are seen for MPS also with slight reduction in percentage variation compared to VMS.

It is observed that deflection for EHP is reduced by 84 to 113% for 4 different elements for BC3 whereas for BC4, EHP exhibits reduced deflection by 30 to 43% only to that of in BC4. The variation in deflection is plotted against the number of elements and shown in Fig. 3.

It can be observed that PP and PPL with HP has shown less deflection and stresses compared to VP. So plates with HP are recommended, unless otherwise required by specific reasons.

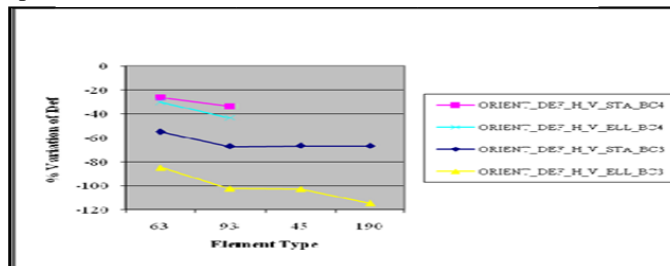


Fig.3: Effect of perforation from horizontal to vertical orientation of unit cell for various elements on deflection represented in terms of percentage.

Table 4: Effect of orientation of perforation on static structural responses for various configurations of unit cell in terms of percentage.

Confg. Element	BC	Orientation of perforation							
		SHP	SVP	% variation	EHP	EVP	% variation		
DEFLECTION $\times 10^{-6}$ m	BC3	SHELL63	0.1213	0.1874	-54.49	0.1207	0.2225	-84.34	
		SHELL93	0.1393	0.2305	-65.47	0.1360	0.2743	-101.69	
		SOLID45	0.1376	0.2271	-65.04	0.1336	0.2700	-102.10	
		SOLSH190	0.1359	0.2241	-64.90	0.1260	0.2695	-113.89	
	BC4	SHELL63	0.6628	0.8381	-26.45	0.6898	0.8997	-30.43	
		SHELL93	0.7831	1.0470	-33.70	0.8113	1.1630	-43.33	
		SHELL63	39.04	66.71	-70.88	43.33	67.70	-52.52	
		SHELL93	51.37	95.82	-86.53	49.72	90.60	-82.22	
	VMS (Pa)	BC3	SOLID45	50.68	94.03	-85.26	49.37	89.10	-80.48
			SOLSH190	47.49	88.97	-87.33	43.97	89.04	-102.72
			SHELL63	90.74	144.04	-58.73	102.26	142.97	-39.81
			SHELL93	119.54	211.00	-76.48	121.93	201.68	-65.41
BC4		SHELL63	43.89	72.13	-64.33	48.54	74.51	-52.42	
		SHELL93	53.87	94.48	-75.38	53.21	93.24	-75.24	
		SOLID45	53.78	93.91	-74.62	53.43	92.60	-73.32	
		SOLSH190	49.77	86.42	-73.62	47.00	92.45	-66.70	
MPS (Pa)		BC3	SHELL63	104.78	163.29	-55.84	117.87	163.50	-38.71
			SHELL93	135.13	223.30	-65.25	138.08	219.46	-58.94

Effect of release of rotation restraint at the boundary nodes

It is observed that deflection for BC3 is reduced 300 to 500% when compared with BC4. The reduction in stresses for BC3 has been found to be 110 to 160% with that for BC4. These percentage variations are arrived from the Tables 4.2 to 4.5 and presented in Table 5 for the entire configuration.

Table 5: Effect of BC3 and BC4 boundary conditions on static structural responses for various configurations of unit cell in terms of percentage.

Confg. Element	BC	Effect of boundary conditions			% Variation	
		SHP	BC3	BC4		
DEF $\times 10^{-6}$ (m)	SHELL63	SHP	0.1213	0.6628	-446.41	
		SVP	0.1874	0.8381	-347.23	
		EHP	0.1207	0.6898	-471.50	
		EVP	0.2225	0.8997	-304.36	
	SHELL93	SHP	0.1393	0.7831	-462.17	
		SVP	0.2305	1.0470	-354.23	
		EHP	0.1360	0.8113	-496.54	
		EVP	0.2743	1.1630	-323.99	
	VMS (Pa)	SHELL63	SHP	39.04	90.74	-132.43
			SVP	66.71	144.04	-115.91
			EHP	43.33	102.26	-134.92
			EVP	67.70	142.97	-111.19
SHELL93		SHP	51.37	119.54	-132.75	
		SVP	95.82	211.00	-120.20	
		EHP	49.72	121.93	-143.25	
		EVP	90.60	201.68	-122.61	
MPS (Pa)		SHELL63	SHP	43.89	104.78	-138.72
			SVP	72.13	163.29	-126.39
			EHP	48.54	117.87	-142.72
			EVP	74.51	163.50	-119.44
	SHELL93	SHP	53.87	135.13	-150.94	
		SVP	94.48	223.30	-136.35	
		EHP	53.20	138.08	-159.51	
		EVP	93.24	219.46	-135.37	

Effect of perforation geometry

It has been found that the former exhibited higher deflection by 0.5 to 7% than the latter for BC3, and reduced by 3 to 4% for BC4 and has been shown in Fig.4.

From Table 6, it is observed that the von Mises stress for BC3 is reduced by 11% for SHELL63 in SHP compared to that in EHP. But the von Mises stresses are higher by 3 to 7% for 8 noded elements model of SHP compared to that of EHP. In BC4, von Mises stress is reduced by 13% for SHELL63 of SHP and reduced by 2% for SHELL93 in SHP.

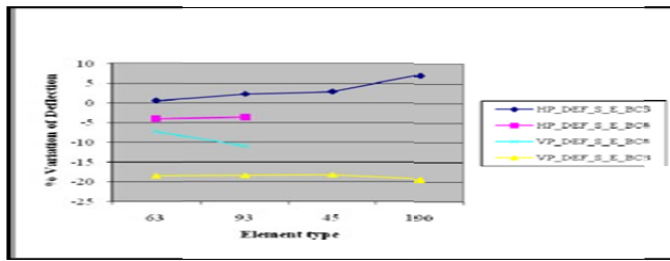


Figure No. 4. Effect of Geometry from slotted to elliptical perforation of unit cell for various elements and terms of percentage

From Table 6, it is observed that the von Mises stress for BC3 is reduced by 1.5% for SHELL63 model of SVP compared to that of EVP whereas for SOLSH190, there is a marginal decrease (0.08%) of stress in SVP. But the stresses are higher by 5 to 6% for SHELL93 and SOLID45 elements in SVP compared to that of corresponding elements in EVP. In BC4, von Mises stress is marginally higher (0.74%) in SHELL63 model of SVP and higher by 4% for SHELL93 model of SVP.

Table 6: Effect of slotted and elliptical geometry of perforation on static structural responses for various configurations of unit cell in terms of percentage.

			SHP	EHP	% Variation	SVP	EVP	% Variation
			Deflection X 10 ⁻⁶ (m)	BC3	SHELL63	0.1213	0.1207	0.49
		SHELL93	0.1393	0.1360	2.37	0.2303	0.2743	-19.00
		SOLID45	0.1376	0.1338	2.91	0.2271	0.2700	-18.89
		SOLSH190	0.1359	0.1260	7.28	0.2241	0.2695	-20.26
	BC4	SHELL63	0.6623	0.6898	-4.07	0.8381	0.8997	-7.35
		SHELL93	0.7831	0.8113	-3.60	1.0470	1.1630	-11.08
		SHELL63	39.04	43.23	-11.30	66.71	67.70	-1.47
		SHELL93	31.37	49.72	3.22	93.32	90.60	5.45
		SOLID45	30.68	49.37	2.80	94.03	89.10	5.27
		SOLSH190	47.49	43.90	7.43	88.97	89.04	-0.08
	BC4	SHELL63	90.74	102.26	-12.69	144.04	142.97	0.74
		SHELL93	119.26	121.93	-1.98	211.00	201.88	4.42
		SHELL63	43.89	48.26	-10.64	72.13	74.20	-3.30
		SHELL93	33.87	33.20	1.23	94.48	93.24	1.31
		SOLID45	33.78	33.43	0.66	93.91	92.60	1.39
		SOLSH190	49.77	47.00	3.57	86.42	92.43	-6.98
	BC4	SHELL63	104.78	117.87	-12.49	163.29	163.30	-0.13
		SHELL93	133.13	138.08	-2.18	223.30	219.46	1.72
		SHELL63	43.892	43.892	0	68.77	68.77	0
		SHELL93	51.87	51.87	0	68.77	68.77	0
	BC3	SHELL63	43.892	43.892	0	68.77	68.77	0
		SHELL93	51.87	51.87	0	68.77	68.77	0
	BC4	SHELL63	43.892	43.892	0	68.77	68.77	0
		SHELL93	51.87	51.87	0	68.77	68.77	0
	BC3	SHELL63	43.892	43.892	0	68.77	68.77	0
		SHELL93	51.87	51.87	0	68.77	68.77	0
	BC4	SHELL63	43.892	43.892	0	68.77	68.77	0
		SHELL93	51.87	51.87	0	68.77	68.77	0

Effect of nodal rotational degrees of freedom of the elements

It is observed from Table 7 that the deflection is reduced by 12%, von Mises stress and maximum principal stress are reduced by 13 to 29% for SHP for BC3 with SHELL63 element compared to SOLID45 and SOLSH190 elements. In case of 8 noded SHELL93element, the above responses are marginally higher than those in SOLID45 and SOLSH190 elements by 2%.

The percentage variation of deflection with respect to element type is shown in Fig. 5. In case of SVP and EVP, the deflection for SHELL63 is reduced by 20% compared to SOLID45 and SOLSH190 and for EHP the deflection is reduced by 5 to 10%. For SHELL93, the deflection for SVP,

EHP and EVP is marginally higher by 2 to 7% compared to that of SOLID45 and SOLSH190.

Table 7: Effect of nodal rotational degrees of freedom of SHELL63 and SHELL93 for various configurations of unit cell on static structural responses in terms of percentage

Effect of nodal rotational degrees of freedom of the elements						
	Configuration	Element No	Element No	Element No	Element No	% Variation
DEF x 10 ⁻⁶ (m)	SHP	SHELL63	0.1213	SOLID45	0.1376	-12.66
		SHELL93	0.1393	SOLID45	0.1338	2.22
		SHELL63	0.1376	SOLSH190	0.1359	2.66
		SHELL93	0.1359	SOLSH190	0.1260	-19.28
	EHP	SHELL63	0.1874	SOLID45	0.2271	-21.18
		SHELL93	0.2303	SOLID45	0.2743	-19.28
		SHELL63	0.2241	SOLID45	0.2695	-2.78
		SHELL93	0.2241	SOLID45	0.2695	-18.69
	EVP	SHELL63	0.1207	SOLID45	0.1260	-0.39
		SHELL93	0.136	SOLID45	0.1338	1.78
		SHELL63	0.2225	SOLID45	0.2700	-21.25
		SHELL93	0.2743	SOLID45	0.2700	1.57
VMS (Pa)	SHP	SHELL63	29.061	SOLID45	30.68	-5.82
		SHELL93	47.49	SOLID45	47.49	-0.00
		SHELL63	51.869	SOLID45	50.68	1.97
		SHELL93	47.49	SOLID45	47.49	0.00
	EHP	SHELL63	66.712	SOLSH190	66.08	0.95
		SHELL93	88.97	SOLSH190	88.97	0.00
		SHELL63	94.03	SOLSH190	94.03	0.00
		SHELL93	94.03	SOLSH190	94.03	0.00
	EVP	SHELL63	43.89	SOLID45	43.89	0.00
		SHELL93	49.72	SOLID45	49.72	0.00
		SHELL63	67.09	SOLID45	67.09	0.00
		SHELL93	67.09	SOLID45	67.09	0.00
MPS (Pa)	SHP	SHELL63	43.892	SOLID45	51.78	-17.29
		SHELL93	51.87	SOLID45	49.77	4.17
		SHELL63	68.77	SOLID45	68.77	0.00
		SHELL93	68.77	SOLID45	68.77	0.00
	EHP	SHELL63	72.129	SOLID45	84.41	-15.80
		SHELL93	93.91	SOLID45	93.91	0.00
		SHELL63	94.477	SOLID45	84.19	11.87
		SHELL93	94.477	SOLID45	84.19	11.87
	EVP	SHELL63	74.507	SOLID45	82.43	-10.82
		SHELL93	89.08	SOLID45	92.43	-4.08
		SHELL63	92.60	SOLID45	92.60	0.00
		SHELL93	92.60	SOLID45	92.60	0.00

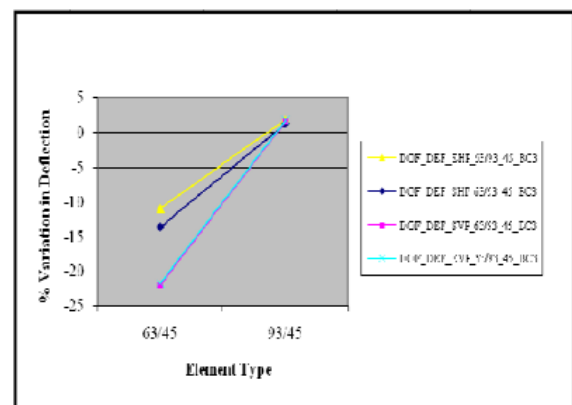


Fig.5: Effect of nodal DOF of SHELL & SOLID45 elements of unit cell on deflection represented in terms of percentage.

Evaluation of Stress concentration and Deflection factor

Stress concentration factor and deflection factor predicted using SHELL63 for slotted and elliptical geometry are compiled and presented in Table 8. This table can be used

as a design support for ligament width of 6 mm since it is based upon under air and water sonar application in India and Russia.

Table 8: SCF and DF of unit cell for various configurations using SHELL63 element.

SHELL63		Stress concentration factor				Deflection factor			
Config-uration	BC	Perforation number							
		1	2	3	4	1	2	3	4
SHP	BC3	2.361	2.286	2.421	7.592	1.436	1.485	1.589	1.554
	BC4	2.487	2.505	2.500	2.256	2.172	2.150	2.248	2.102
SVP	BC3	4.188	5.546	3.682	4.248	2.256	2.144	2.284	1.845
	BC4	5.248	3.568	3.256	3.259	2.482	2.756	2.614	2.658
EHP	BC3	1.802	1.568	1.954	4.654	1.564	1.559	1.706	1.547
	BC4	2.624	2.348	2.654	3.351	2.225	2.246	2.206	2.528
EVP	BC3	6.056	8.685	5.258	6.254	2.896	2.685	2.524	2.400
	BC4	6.002	4.258	5.357	4.152	3.256	3.254	3.112	2.566
SHP of PPL	BC3	2.500	2.356	2.651	6.256	1.669	1.568	1.571	1.628
	BC4	2.105	2.150	2.359	8.145	1.248	1.256	1.270	1.262
SVP of PPL	BC3	4.388	4.231	4.625	4.426	2.489	2.148	2.174	1.748
	BC4	3.562	13.10	3.536	6.102	1.865	1.562	1.564	1.658
EHP of PPL	BC3	2.371	1.806	2.256	2.356	1.455	1.456	1.548	1.214
	BC4	1.708	1.786	2.652	3.035	1.299	1.239	1.248	1.265
EVP of PPL	BC3	5.150	3.200	4.248	4.625	2.498	2.248	2.112	1.224
	BC4	4.216	8.022	3.659	7.771	1.865	1.556	1.658	1.281

Considering SCF and DF, it is to observe that for SHELL63 for BC3, EHP shows reduced stress concentration factor and SHP shows reduced deflection factor around its periphery of the perforation. This is due to the presence of geometric discontinuities existing at the locations of perforations in PPL.

V. CONCLUSION

Finite element results for NPP have been compared with the exact solution inspection and it is found that principal stress predicted by SHELL63 elements is lower by 1.27%. For the SHELL93, the reduction in stress is predicted by 1.2% compared to the exact solution. However the reduction in stress for the SOLID45 and SOLSH190 is found to be 1.32% compared with the exact solution. There is only marginal difference in stress between SHELL63 and SHELL93. This implies that SHELL93, which is an eight noded element will lead to a finite element model of the plate with more number of nodes than SHELL63 which is a four noded element and the analysis if performed with SHELL63 will give somewhat the same quality results as SHELL93 at a reduced computational effort. Considering these facts, the number of nodes and elements and computational effort, SHELL63 is recommended for the analysis.

The static responses viz., deflection, VMS and MPS for SHP and EHP are lower than that of SVP and EVP, for both the boundary conditions and for all the four elements used in the modeling. Hence horizontal perforation orientation is recommended for application. The horizontal orientation should be along the smaller dimension of the plate as analyzed in this investigation.

Deflection, VMS and MPS of SHP and EHP for BC3 are lower than the corresponding values of BC4. This state is as expected since BC3 has all the rotations restrained along with translations. The 5 to 10% variation in the deflection and stresses is likely to surface out, when the actual fixed edge cannot provide the full fixity expected from that as in the case of a defective weld.

Horizontal perforation and BC3 boundary condition are the recommended feature of the PP. SHP gives 5% higher deflection than EHP, whereas the VMS and MPS predicted in SHP is lower than that in EHP. Based on the studies on unit cell of two configurations, two perforations and four types of elements, it is recommended to use SHP for the under air and water applications and SHELL63 element for further numerical investigations

REFERENCES

- [1] G. Kirsch, "Plane stress solution for a thin plate of infinite width with a hole under tension" VDI Vol. 42, 1898, pp.797-807.
- [2] G. B. Jeffery, "Plane stress and plane strain in bi-polar coordinates" Phil. Trans. of the royal sec. Series A.221, London (1921), pp. 268-390.
- [3] R. C. J. Howland, "One the stresses in the neighborhood of a circular hole in a strip under tension." Phil. Trans. A 229,1929, pp.49-86.
- [4] A. A. Sokolov, "The elastic plastic state of a plate", Doki. Akad. Mask SSR, Vol.x, No. 1,1948.
- [5] I. I. Feverberg, "Tension applied to a plate with a circular hole with stresses exceeding the limit of elasticity", Trudy, Ixst, No. 615(1947).
- [6] N. Merketos,"Elastic plastic analysis of perforated thin strip of a strain hardening material", Int. J. Mech. Phys. Solids, vol. 12, 1964, pp. 370.
- [7] P. V. Maroal and J.P. King," Elastic plastic analysis of two dimensional stress system by the finite element method", Int. J. Mech. Vol. 9, 1967, pp.143.
- [8] S. B. Griffith, "Experimental investigation of the effect of plastic flow in a tension panel with a circular hole", NACA, TB 1705, 1940.
- [9] S. N. Ibrahim and Mc.Callion, "Elastic plastic deformation around a circular hole in a plate under cyclic loading",Appl. Mech.
- [10] Convention, 1966. Int. J. Mech. Eng. London, Proc. 1965-66, Vol. 180, Part 31, pp. 438-447.
- [11] G. Cookerhers and D. H. Baton, "An estimation of plastic zones in a plate with central hole", Strain, Vol. 12, No. 4, Oct. 1976, pp. 145-150.
- [12] C. V. Byre Gowda and T. N. Topper, "On the relation between stress and strain concentration factor in a notched

- member in a plane stress”, J. Appl. Mech., Vol. 37, No. 1, March 1970, pp. 77-84.
- [13] W. A. Box, “The effect of the plastics strains on the stress concentrations”, Proc. SESA. Vol. 8, No. 2, 1950, pp. 999-1010
- [14] ISO 3411 physical dimensions of operators ISO 4254-1:2013 - Agricultural machinery - Safety -Part1 Ansys mechanical’s userguide
- [15] M. AydinKomur, “Elasto-plastic buckling analysis for perforated steel plates subject to uniform compression”, Mechanics Research Communications 38 (2011)117–1220.
- [16] G.N. Savin, “Stress Concentration around Holes”, Pergamon Press, New York(1961)
- [17] Jae-Hoon Kang, “Exact Solutions of Stresses, Strains, and Displacements of a Perforated Rectangular Plate by a Central Circular Hole Subjected to Linearly Varying In-Plane Normal Stresses on Two Opposite Edges”, International Journal of Mechanical Sciences,2014
- [18] Jinho Wool and Won-Bae Na1, “Effect of Cutout Orientation on Stress Concentration of Perforated Plates with Various Cutouts and Bluntness” International Journal of Ocean System Engineering 1(2) (2011)95-101
- [19] Emanuele Maiorana, Carlo Pellegrino, Claudio Modena, “Elastic stability of plates with circular and rectangular holes subjected to axial compression and bending moment”, Thin-Walled Structures 47 (2009) 241–255
- [20] D.B.Kawadkar, Dr.D.V.Bhope, S.D. Khamankar “Evaluation of Stress Concentration in Plate with Cutout and its Experimental Verification”, International Journal of Engineering Research and Applications (IJERA) ISSN: 2248-9622, Vol. 2, Issue5, September- October 2012, pp.566-571
- [21] J. Rezaeepazhand, and M. Jafari, “Stress Analysis of Perforated Composite Plates, Composite Structures”, 71 (3-4) (2005) 463-468. The Industrial Perforators Association.
- [22] R. Nandagopan, S. Ranjith Kumar, M.R. Rajesh, K. Manoharan, and C.G. Nanda kumar, “Nonlinear Behaviour of Perforated Plate with Lining” Defence Science Journal, Vol. 62, No. 4, July 2012, pp. 248-251